Dynamic Life Cycle Economic and Environmental Assessment of Residential Solar Photovoltaic Systems

1. Introduction

Over the last decade, solar PV energy generation in the US has increased substantially, primarily driven by cost reduction (Verlinden et al., 2013) as well as concerns related to greenhouse gas and air pollutant emissions (Azzopardi and Mutale, 2010). Around 92.6 TWh of solar PV energy was generated across the US in 2018, representing 2.2% of the nation's total electricity generation and 12.5% of the total renewable energy generation (EIA, 2019a, 2019b). Specifically, around 32% of this energy was generated by small-scale distributed solar PV systems that are commonly found on residential and commercial rooftops (EIA, 2019b), while the remaining was generated at utility scale facilities. Cost reduction has been one of the major drivers for the increased adoption of distributed solar PV systems. It has been estimated that a 63% drop in the residential PV manufacturing and installation cost has taken place since 2010, with an average cost of $2.70 per Watt DC in 2018 (Fu et al., 2018). The cost of solar PV systems is often positively related to the system capacity or size (Fu et al., 2018). Larger systems are likely to have higher upfront costs, and hence impose a greater financial burden on individual households (Nelson et al., 2006). Yet such systems may create a higher environmental benefit when the generated solar energy can be fully utilized by the household or sold to the grid (Kaundinya et al., 2009). Therefore, it is imperative to understand the economic and environmental tradeoffs of the distributed solar PV systems to inform their co-optimization.

The economic performance of solar PV systems is often assessed through life cycle cost assessment (LCCA), which accounts for all costs and savings that incur during the life span of the PV systems (Rebitzer et al., 2004), utilizing indicators such as levelized cost of electricity (LCOE) (e.g., Allouhi et al., 2019, 2016; Burns and Kang, 2012; Jones et al., 2018; Kazem et al., 2017; Lai and McCulloch, 2017; Zhang et al., 2016), investment payback time (IPBT) (e.g., Berwal et al., 2017; Chandel et al., 2014; Lee et al., 2018;

Poullikkas, 2013), and life cycle cost (e.g., Adriana et al., 2012; Akinyele and Rayudu, 2016a, 2016b; Bortolini et al., 2014; De Souza et al., 2017; Gürtürk, 2019; Uddin et al., 2017). Meanwhile, their environmental performances are often examined through life cycle assessment (LCA), which is a methodological framework that assesses environmental impacts attributable to the entire life cycle of a product (Rebitzer et al., 2004). The common types of environmental impacts that have been studied via previous solar PV LCAs include carbon footprint (e.g., Akinyele et al., 2017; Akinyele and Rayudu, 2016a, 2016b, Allouhi et al., 2019, 2016; Jones et al., 2018; Rawat et al., 2018; Xu et al., 2018) and cumulative energy demand (CED) (e.g., Gerbinet et al., 2014; M. Raugei, 2015; Peng et al., 2013; Rawat et al., 2018; Tsang et al., 2016; Wu et al., 2017). Not many studies have evaluated solar PV systems from both economic and environmental perspectives to allow understandings of their tradeoffs. Indeed, tradeoffs in solar PV systems' economic and environmental performances exist when comparing different types of PV system designs for a particular application (Allouhi et al., 2019, 2016; Jones et al., 2018) and integrating solar PVs into grids with different energy mixes (Bernal-Agustín and Dufo-López, 2006). However, such tradeoffs have not been fully investigated for different solar PV and battery sizing scenarios under both the grid-connected (GC) and standalone (SA) contexts.

Furthermore, many of the previous solar PV LCCAs and LCAs have limited consideration of the dynamic diurnal or seasonal patterns of solar power generation and demand (Adriana et al., 2012; Chandel et al., 2014; De Souza et al., 2017; Rawat et al., 2018). Such dynamic patterns, however, are important in informing management actions as well as regulatory incentives, including battery dispatch strategies, time-of-use rates, net metering, and energy and water conservation practices. Studies utilizing static or averaged solar energy generation or demand data were limited in their transferability to different spatial and temporal conditions. Of the studies that did include dynamic solar power generation and/or demand patterns, Kazem et al. (2017) estimated the generation potential of a grid-connected 1-MW power plant in Adam, Oman in offsetting peak load using local hourly solar radiation, humidity, temperature, and wind speed data (Kazem et al., 2017). Lee et al. (2018) used hourly solar radiation and building energy consumption data to estimate

the economic potential of grid-connected rooftop PV systems for each building in Seoul, South Korea (Lee et al., 2018). Uddin et al. (2017) examined the influence of battery degradation on the technical and economic performances of solar PV systems, using a residential mid-sized family house in the UK as a case study. While these studies provided important insights into the influence of dynamic solar generation and demand patterns on the PV systems' economic performances, the environmental performances of solar PV systems were excluded. Very few studies have included the dynamic solar energy generation and consumption patterns in assessing the life cycle environmental outcomes of the solar PVs. Akinyele et al. (2016a, 2016b) combined a process-based load demand model with LCCA and LCA to evaluate the technical, economic, and environmental (i.e., carbon emissions) performances of SA PV systems in off-grid communities in Nigeria. They found the proposed PV systems could meet as much as 99.56% of the demand, while performing better both economically and environmentally than conventional diesel power plants. Jones et al. (2018) developed a spreadsheet model to simulate hourly electricity flows into and from a non-domestic building in UK under three system configurations: no solar PV installed, solar PV alone, and solar PV combined with battery storage. The model was then combined with LCA and discounted cash-flow analysis to assess the carbon emissions and the net present values associated the three system configurations. Neither of these studies, however, investigated the influence of panel and battery sizing on PV systems' performances. Additionally, HOMER (Hybrid Optimization of Multiple Energy Resources) is a popular tool that can be used to assess both the technical-economic and environmental performances of solar PV systems. However, the environmental impacts assessed through HOMER are limited to the use phase of the solar PV systems.

Building upon these previous modeling efforts, this study seeks to develop a comprehensive and generalizable modeling framework to capture the dynamic life cycle economic and environmental performances of solar PV systems. A system dynamics model (SDM) of distributed residential solar PV systems was developed and combined with LCA and LCCA to evaluate the environmental and economic tradeoffs of GC and SA solar PV systems under different panel and battery sizing scenarios. The SDM

framework was selected based upon its capability to be adapted to various spatial and temporal conditions as well as to visualize the detailed system processes. The modeling framework was demonstrated using a prototype house in Boston, MA of the United States. This study aims to test the following two hypotheses: 1) environmental and economic tradeoffs exist when optimizing the panel and battery sizes for the SA solar PV system, but not for the GC system; and 2) there are optimal panel and battery sizes that can simultaneously optimize the percent demand met and the life cycle cost of the SA solar PV systems.

2. Methodology

The modeling framework developed in this study combines LCA and LCCA with SDM. SDM is a computational approach applying linked differential equations to simulate the behavior of complex systems over a certain time period. It has been recognized as a cogent tool to study interactions among system components by capturing system feedback loops and delays (Forrester, 1997; Sterman, 2000). Life cycle phases considered in this study include manufacturing, transportation, and use phases. The end-of-life phase was neglected because of the low total amount, concentration and value of reclaimable material in collecting and recycling solar cells (Spanos et al., 2015). The manufacturing and transportation phases of the solar PV systems were assessed based upon unit costs and emission rates associated with individual solar PV components through conventional LCCA and LCA. The use phase was modelled through SDM. Particularly, SDM was used to dynamically simulate the solar energy generation, demand, and storage processes during the use phase of solar PV systems. The modeling framework enables assessment of the net present value (NPV), CED, carbon footprint, and water footprint of solar PV systems over their life span. Figure 1 illustrates the modeling framework developed in this study.

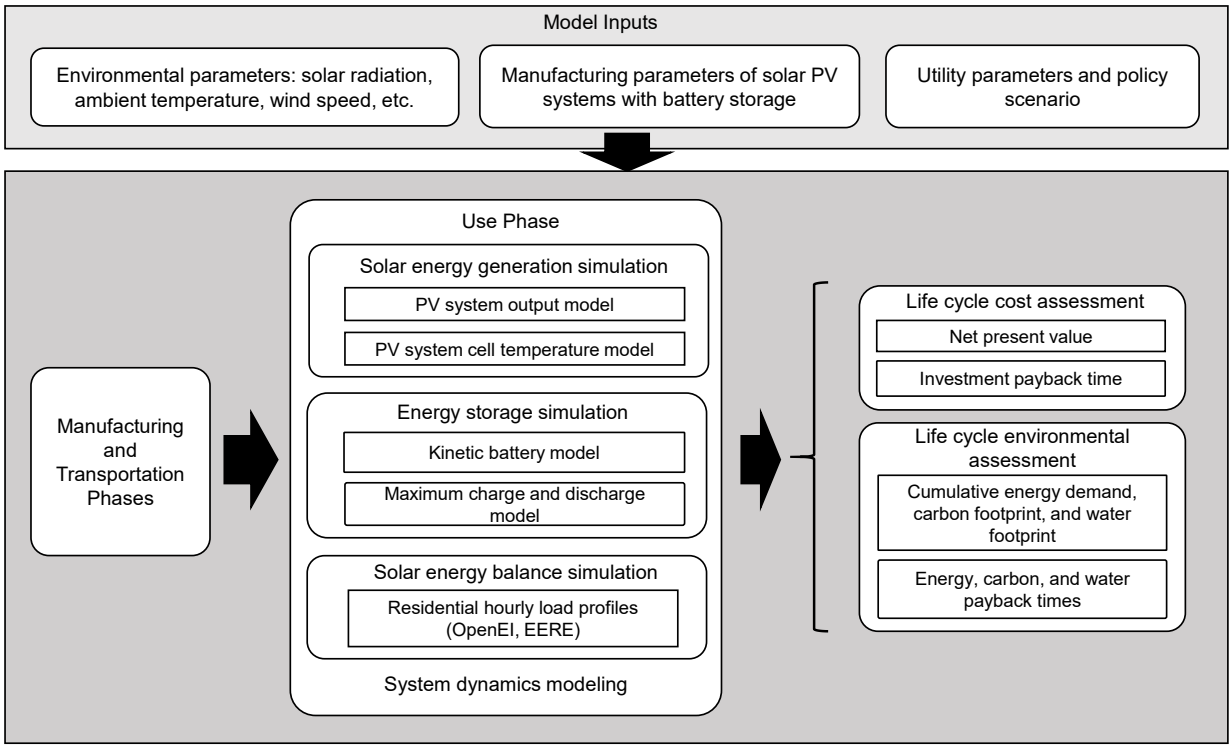

Figure 1. Modeling framework for the dynamic life cycle assessment of solar PV systems

2.1 System description

This study focuses on polycrystalline silicon (poly-Si) solar PV systems based upon their popularity and economic competitiveness (Fthenakis and Kim, 2011; Sharma et al., 2015). The system investigated in this study consists of solar panels (composing PV array) (poly-Si), balance of system (BOS), and energy storage (if any) (Parida et al., 2011). BOS includes inverters, electrical wiring, mountings, and meters. We assumed that the size of the solar panels was not constrained by the roof size. Two system settings were examined: GC and SA systems (Figure 2). GC system uses the grid as a supplement to the solar energy generated onsite and allows users to sell surplus solar energy to the grid (Elhodeiby et al., 2011). SA system refers to an off-grid solar PV system that does not allow selling of surplus energy (Abu-jasser, 2010).

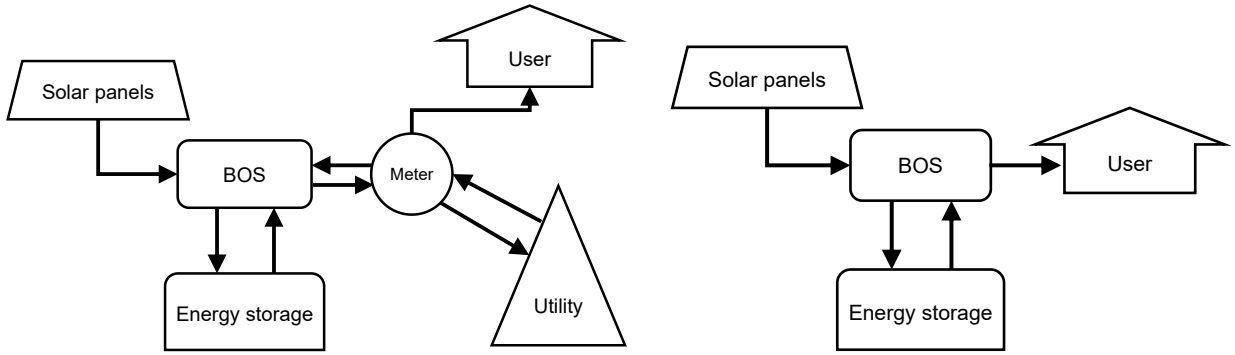

Figure 2. Sketch of the designs of the grid-connected (GC; left) and standalone (SA; right) solar PV systems that were investigated in this study

Boston, MA was selected as a testbed in our study because of its high electricity price (EIA, 2017), strong in-place solar incentive programs (Eid et al., 2014; Heeter et al., 2014), and its active pursue of renewable energy (Burns and Kang, 2012). Currently, around 10.7% of the state's electricity comes from solar energy (EIA, 2019c). The solar energy capacity for power generation is projected to grow to 1,603 MW over the next 5 years (SEIA, 2019). Boston has an average solar energy potential of around 4.48 kWh/m^2/day (DOE, n.d.), with July being the highest (5.86 kWh/m^2/day) and December being the lowest (1.60 kWh/m^2/day) (NREL, 2015). Boston has a continental climate with warm summers and cold and snowy winters (Kottek et al., 2006). The annual average ambient temperature of Boston is around 10.5 °C, with the lowest temperature of -21.14 °C in January and the highest of 36.02 °C in July (NREL, 2015). The annual average wind speed in Boston is around 0.89 m/s, with the lowest wind speed of 0.01 m/s in July and the highest of 2.45 m/s in February (NREL, 2015).

A prototype low-rise multifamily house with five housing units based upon the US Department of Energy's House Simulation Protocol was used for model application (Wilson et al., 2014). An hourly energy demand profile specific to the multifamily house in Boston, MA was obtained from the Open Energy Information database (NREL, 2014) and each data point was then divided into equal halves to achieve 30-minute simulation. Typical baseline SA and GC PV systems with 40 panels (1.63 m^2/panel) and 40 batteries (1.02

kWh$_c$/battery) in each system was simulated on a 65 m^2 rooftop in the model. The 40-panel PV system's capacity was assumed to be sufficient enough to cover the peak load of demand in the selected house with the consideration of future electrification applications like electric vehicles. The 40-battery storage was calculated to cover the average daily demand of the house based on the energy demand profile.

2.2 System dynamics modeling of the solar PV system

The system dynamics model was developed using the Vensim DSS® software. Vensim DSS® is a powerful simulation tool for developing, analyzing, and visualizing dynamic feedback models (Ventana Systems, 2015). It has wide applications in management (Sterman, 2000) and environmental studies (Ford and Ford, 1999) to support decision-making. This model includes three main components: solar energy generation, storage, and balance simulations (Figure 3). Details of each component are provided in the following sub-sections. The simulation ran over one year with a thirty-minute time step, which is typical among previous renewable energy system simulation efforts (Connolly et al., 2010).

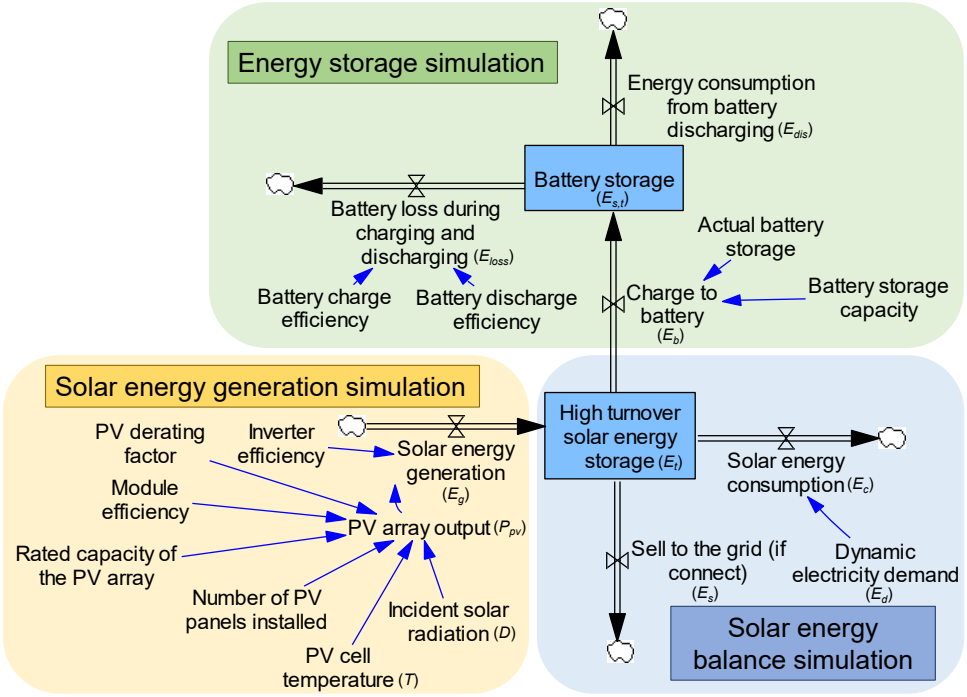

Figure 3. A simplified structure of the system dynamics model of the solar PV systems

148 2.2.1 Solar energy generation simulation

149 The output of PV array (P_{pv}, kW) was simulated based upon Equation 1. Specifically, the 30-minute solar
150 radiation profile for the City of Boston was obtained from the National Solar Radiation Database (NREL,
151 2015) and used to calculate the incident solar radiation (D, kW/m^2) at each time step. The average residential
152 panel size (S) and the PV module efficiency (β) indicate the rated capacity of a PV panel, which were
153 assumed to be 1.63 m^2 and 15% (NREL, 2017). The number of PV panels installed (n) was simulated. A
154 PV derating factor (f_{pv}) of 95% was used (HOMER, 2017). An hourly degradation rate (f_d) of the PV
155 system was calculated based upon the annual degradation rate of 0.5% obtained from Köntges et al. (2016).
156 The temperature coefficient of power (α) indicates the influence of the PV cell temperature on the system
157 efficiency, which was assumed to be -0.48 %/°C (HOMER, 2018). The incident radiation at standard test
158 conditions (D_{STC}) and the PV cell temperature under standard test conditions (T_{STC}) were assumed to be 1
159 kW/m^2 and 25 °C respectively (HOMER, 2017).

160

161 $$P_{pv,t} = S\beta n f_{pv}\left(\frac{D_t}{D_{STC}}\right)[1 + \alpha(T_t - T_{STC})]\,(1 - f_d)^t \quad \cdots\cdots \text{Equation 1}$$

162

163 Where,

164 $P_{pv,t}$ represents the actual output of the PV array in the current time step, kW;

165 t is a time step index, which goes from 0, 0.5, up to 8759.5;

166 S is the average residential panel size, 1.63 m^2 (length: 65 inches, width: 39 inches);

167 β is the PV module efficiency, 15%;

168 n is the number of PV panels installed;

169 f_{pv} is the PV derating factor, 95%;

170 D_t is the incident solar radiation on the PV array in the current time step, kW/m^2 (NREL, 2015);

171 D_{STC} is the incident radiation at standard test conditions, 1 kW/m^2;

172 α is the temperature coefficient of power, -0.48 %/°C;

173 T_t stands for the PV cell temperature in the current time step, °C;

174 T_{STC} is the PV cell temperature under standard test conditions, 25 °C;

175 f_d is the hourly degradation rate of the PV system, 0.000057%.

176

177 The PV cell temperature (T, °C) was further calculated using Equation 2 (Duffie and Beckman, 1991;
178 HOMER, 2018). Ambient temperatures in Boston at 30-min intervals (T_a, °C) were obtained from the
179 National Solar Radiation Database (NREL, 2015). In addition, the Sandia Module Temperature Model
180 (SNL, 2018) (Section 2 of the SI) and Faiman Module Temperature Model (Faiman, 2008) (Section 2 of
181 the SI) were used to validate results obtained from Equation 2.

182

183
$$T = \begin{cases} \dfrac{T_a + \left(T_{pv,NOCT} - T_{a,NOCT}\right)\left(\dfrac{D}{G_{T,NOCT}}\right)\left[1 - \dfrac{\eta_{mp,STC}(1 - \alpha T_{STC})}{\tau\alpha_b}\right]}{1 + \left(T_{pv,NOCT} - T_{a,NOCT}\right)\left(\dfrac{D}{G_{T,NOCT}}\right)\left(\dfrac{\alpha\eta_{mp,STC}}{\tau\alpha_b}\right)}, & D > 0 \\ T_a, & D = 0 \end{cases}$$

184 ··· ··· Equation 2

185

186 Where,

187 T represents the PV cell temperature in the current time step, °C;

188 T_a is the ambient temperature in the current time step, °C;

189 $T_{pv,NOCT}$ is the nominal operating cell temperature, 46.5 °C (HOMER, 2017);

190 $T_{a,NOCT}$ is the ambient temperature at which the NOCT is defined, 20 °C (García and Balenzategui, 2004;
191 Koehl et al., 2011);

192 D is the solar radiation striking the PV array in the current time step, kW/m^2 (NREL, 2015);

193 $G_{T,NOCT}$ is the solar radiation at which the NOCT is defined, 0.8 kW/m^2 (García and Balenzategui, 2004;
194 Koehl et al., 2011);

195 $\eta_{mp,STC}$ is the maximum power point efficiency under standard test conditions, 13% (HOMER, 2017);

α is the temperature coefficient of power, -0.48 %/°C (NREL, 2017);

T_{STC} is the cell temperature under standard test conditions, 25 °C (Devices—Part, 1AD; Muñoz-García et al., 2012);

τ is the solar transmittance of any cover over the PV array, 90% (Duffie and Beckman, 1991);

α_b is the solar absorptance of the PV array, 90% (Duffie and Beckman, 1991).

2.2.2 Energy storage simulation

Battery energy storage system was simulated based upon Equation 3. Generic Li-Ion battery was modelled with information obtained from (HOMER, 2017). The amount of energy available in the battery system ($E_{s,t}$, kWh) was modeled as a stock, which is a time integral of differences between the rate of solar power charged to the battery (E_b, kW), the rate of battery discharges for end uses (E_{dis}, kW), and the rate of battery loss during charging and discharging (E_{loss}, kW). The initial battery storage ($E_{s,\,t_0}$) was assumed to be zero. The rate of charging (E_b) is determined by the PV array output (P_{pv}), the user's energy demand, as well as the vacant capacity of the battery system at a given time step. The rate of discharging (E_{dis}) is determined by the battery storage and the user demand. The rate of battery loss (E_{loss}) is determined by the battery charge and discharge efficiency. Furthermore, both E_b and E_{dis} are constrained by the maximum rates which were calculated using the Kinetic Battery Model (HOMER, 2017; Manwell and McGowan, 1993) with consideration of the battery storage and charge current limitations. Details about the calculation of the maximum charging and discharging rates are provided in the Section 2 of the SI.

$$E_{s,t} = \int_{t_0}^{t} (E_b - E_{dis} - E_{loss})\, dt + E_{s,\,t_0} \cdots \cdots \text{Equation 3}$$

Where,

E_b is the charge to the battery, kW;

E_{dis} is the discharge of electricity energy from the battery, kW;

E_{loss} is the battery loss during charging and discharging, kW;

$E_{s,t}$ and $E_{s,\,t_0}$ are the energy storage in battery at time *t* and t_0, kWh.

The useful battery lifespan (T_b, year) was calculated based on the total lifetime throughput of the battery system and the annual actual charge-discharge throughput (Equation 4). The lifetime throughput of one battery was assumed to be 2,430 kWh (HOMER, 2018), and total throughput was assumed to be linearly related to the number of batteries in the system. The actual annual charge-discharge throughput of the battery storage (C_a) was calculated as a time integral of the charging rate (Spanos et al., 2015).

$$T_b = \frac{C_l m}{C_a} \quad \cdots\cdots \text{Equation 4}$$

Where,

T_b represents the actual useful lifespan of the battery storage, year;

C_l is the lifetime throughput of one battery, 2,430 kWh;

m is the number of batteries installed in the battery system;

C_a is the actual annual charge-discharge throughput of the battery storage, kWh/year.

2.2.3 Solar energy balance simulation

The dynamic energy balance between solar energy generation, battery storage, consumption, and selling to the grid was simulated based upon Equation 5. A fictitious high turnover stock was simulated to allocate the generated solar energy (E_g) to the three outflows, E_c, E_b, and E_s (Equation 6).

$$E_t = \int_{t_0}^{t} \left(E_g - E_c - E_b - E_s\right) dt + E_{t_0} \quad \cdots\cdots \text{Equation 5}$$

$$E_g\ (\text{inflow}) = E_c + E_b + E_s\ (\text{outflow}) \quad \cdots\cdots \text{Equation 6}$$

Where,

E_t and E_{t_0} are the solar energy storage at time t and t_0, kWh;

E_g is the solar energy generation by the PV system, kW;

E_c is the solar energy consumption to meet the demand, kW;

E_b is the solar energy for charging the battery storage, kW;

E_s is the solar energy that feeds into the grid, kW.

The decision-making process for the solar energy generated to be allocated to the three outflows is illustrated in Figure 4. Whenever solar energy is available, it is first used to meet the household energy demand. The surplus solar energy is used to charge the battery if it is present and has not reached the maximum capacity. After the battery is fully charged, the excess solar energy is sold to the grid through net metering.

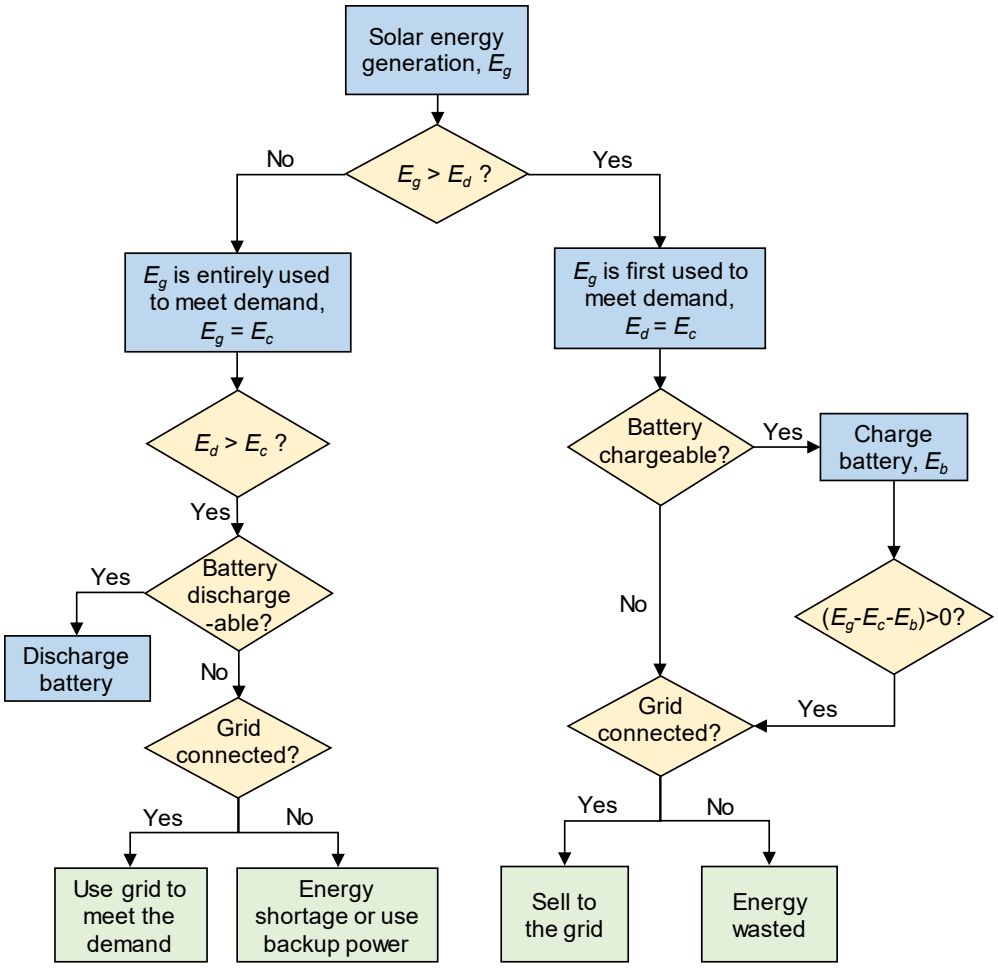

Figure 4. Solar energy balance simulation decision flow (E_g is the solar energy generation by the PV system, kW; E_c is the solar energy consumption to meet the demand, kW; E_b is the solar energy for charging the battery storage, kW; and, E_d is the electricity demand in current time step, kW.)

2.3 Life cycle cost assessment

The life cycle cost of installing solar PV systems was determined by the capital cost of the PV systems, savings from solar energy generation, tax credit and rebate, cost of labor and the annual operation and maintenance (O&M) cost (Equation 7). A 20-year life cycle cost was calculated based upon the initial net cost and annual net cost (i.e., annual O&M cost subtracts annual savings from solar energy generation) accumulated to 20 years. All future costs were discounted to the year of 2018 applying a typical discount rate of 5% (Jeong et al., 2019; Leckner and Zmeureanu, 2011; Shea et al., 2020). The capital cost of the PV

system includes costs related to battery, panels and racking, inverters, permission, and installation. The cost of battery storage was assumed to be \$209 per kWh of storage capacity (kWh_c) (Curry, 2017). Panels and racking were assumed to cost \$1 per Watt of generation capacity (McFarland, 2014; Reichelstein and Yorston, 2013). Inverters were assumed to be \$300 per piece (HOMER, 2018). Permission and installation cost including meters were assumed to be \$450 (NREL, 2017). Savings from solar energy generation were calculated as a product of the cumulative amount of solar energy that is consumed and/or sold to the grid and the electricity retail price. The electricity rate was assumed to be \$0.16/kWh, which is the average flat rate in New England area from 2016 to 2017 (NREL, 2017). A tax credit of 30% (Burns and Kang, 2012; Service, 2019) of the capital cost was applied. In addition, a rebate of \$0.25 per Watt of installed capacity was applied to all solar systems (Association, 2015). The cost of labor is a tiered function of the system capacity, which was obtained from (HomeAdvisor, 2019) (Figure S1 in the Section 2 of SI). The cost of O&M includes the annual replacement cost of battery storage during the system life cycle. The interconnection costs (e.g. application fees) of GC system were neglected (Eversource, 2018). Investment Payback Time (IPBT) of the PV systems was calculated using a cash flow method using Equation 8.

$$Life\ cycle\ cost = C_c - R + \sum_{n=1}^{N} \frac{C_{o,n}}{(1+i)^n} - \sum_{n=1}^{N} \frac{S_n}{(1+i)^n} \quad \cdots\cdots \text{Equation 7}$$

$$\text{IPBT} = T_y + \frac{-v}{p} \quad \cdots\cdots \text{Equation 8}$$

Where,

C_c is the capital cost of the PV systems, \$;

R is the tax credit and rebate, \$;

N is the life span of the solar PV systems, 20 years;

$C_{o,n}$ is the O&M cost in the year n, \$;

i is the discount rate, 5%;

296 S_n is the saving from solar energy generation in the year n, \$;

297 T_y is the number of years after the initial investment at which the last negative value of cumulative cash

298 flow occurs, year;

299 p is the net cash flow within the year when the first positive value of cumulative cash flow occurs, \$/year;

300 v is the cumulative cash flow up to the year at which the last negative value of cumulative cash flow

301 occurs, \$.

302

303 2.4 Life cycle environmental assessment

304 Three types of environmental impacts were simulated: CED, carbon footprint, and water footprint. The

305 system boundary includes manufacturing, transportation, installation, and use phases. The environmental

306 costs related to labor and administration during the use phase were neglected. However, the replacement of

307 batteries was included. Due to various disposal behavior of the PV users as well as no regulation on the

308 residential level for separating batteries from PV systems and disposing the systems, the battery disposal is

309 not included (Grinenko, 2018). SimaPro 8.3 was used for characterization of the environmental impacts.

310 Particularly, the cumulative energy demand V1.09 method was used for estimating CED. The IPCC 2013

311 GWP 20a was used for estimating carbon footprint. No significant difference was found in model output

312 applying the IPCC 2013 GWP 20a or 100a. The Berger et al 2014 (Water Scarcity) method was used for

313 estimating water footprint (Boulay et al., 2018). Environmental savings from solar energy generation during

314 the use phase were calculated as a product of the cumulative amount of solar energy that is consumed and/or

315 sold to the grid and the environmental impacts units. Equation 9 is the governing equation of the solar PV

316 systems' life cycle environmental performance. Energy, carbon, and water payback time were calculated

317 using Equation 10. Table 1 presents the unit costs and environmental impacts obtained from SimaPro 8.3.

318

319 $$I = I_{t_0} + I_s - \int_{t_0}^{t} (P_{pv}\, f_{unit})\, dt \quad \cdots\cdots \text{Equation 9}$$

320

Where,

I and I_{t_0} are the cumulative environmental costs at time t and t_0;

I_s is the environmental costs of the PV system (from cradle to gate without the solar generation savings);

P_{pv} is the actual output of the PV array in the current time step, kW;

f_{unit} is the environmental impacts unit, environmental impacts/kWh, Table 1.

$$\text{PBT} = \frac{E_p + E_t}{E_g - E_m} \quad \cdots\cdots \text{Equation 10}$$

Where,

PBT represents the environmental payback time, which can be either energy, carbon, or water payback time, year;

E_p is the environmental cost to produce and manufacture the solar PV system;

E_t is the environmental cost to transport materials used during the life cycle;

E_g is the average annual environmental savings from electricity generation by the installed solar PV system;

E_m is the average annual environmental cost of O&M including the battery replacement.

Table 1. CED, carbon footprint, water footprint and cost unit of solar PV systems

Solar PV systems	SimaPro entry	CED unit	Carbon footprint unit	Water footprint unit	Cost unit
PV panel	Photovoltaic panel, multi-Si wafer {GLO}| market for | Alloc Def, S	3480 MJ/m^2	202 kg CO_2 eq/m^2	4360 L/m^2	\$1/W
Battery	Battery, Li-ion, rechargeable, prismatic {GLO}| market for | Alloc Def, S	96.5 MJ/kg	7.52 kg CO_2 eq/kg	101 L/kg	\$209/ kWh_c
Inverter	Inverter, 2.5kW {GLO}| market for | Alloc Def, S	2400 MJ/piece	243 kg CO_2 eq/ piece	1910 L/piece	\$300/ piece

Meter and wiring	Not considered				$450
Replaced grid electricity	Electricity, at grid, US/US, kWh	10.9 MJ/kWh	0.878 kg CO_2 eq/kWh	44.1 L/kWh	$0.16/ kWh

338

339 2.5 Sensitivity analysis

340 A sensitivity analysis was conducted to analyze the influence of discount rate and the local electricity grid
341 mix on the environmental and economic outcomes of the typical GC and SA PV systems with 40 panels
342 and 40-batteries. Each of these factors were varied by ± 10, 30, 50, 70, 90, and 100% to assess its influence
343 on the NPV, CED, carbon footprint, and water footprint. A sensitivity index (S) was calculated for each
344 input change using Equation 11 (Song et al., 2019).

345 $$S = \frac{\frac{O_i - O_b}{O_b}}{\frac{I_i - I_b}{I_b}} \quad \cdots\cdots \text{Equation 11}$$

346 Where O_i is the output value after the input was changed; O_b is the base output value; I_i is the altered input
347 value; and I_b is the original input value. Inputs were considered "highly sensitive" if $|S|$ >1.00.

348

349 **3. Results and Discussion**

350 3.1 Solar energy utilization and demand met by SA and GC PV systems

351 For the prototype house with 40 PV panels and 40 batteries, 42.6% of the solar energy generation is directly
352 consumed and 44.4% is stored for later consumption. Around 13.0% of the solar energy will either be
353 wasted in a SA system or sold to the grid in a GC system. Solar energy generated, stored, and sold/wasted
354 all present strong seasonal trends (Figure 5). Solar energy generation peaks between May and July, when
355 the monthly average energy demand of the prototype house is the lowest. Hence, a larger amount of solar
356 energy can be sold or stored during these months. Furthermore, grid demand is the highest during summer
357 months nationally (EIA, 2011). Utilities often use natural gas (71.5% in the New England region), hydro
358 and nuclear generation to meet the additional demand (ISO-NE, 2018). Installation of a GC PV system can

hence alleviate local energy stress and replace fuels that have higher carbon emission factors. Nevertheless, the opposite seasonal patterns of solar energy demand and generation will not be ideal for households looking to install SA PV systems. More solar energy is likely to be wasted and a larger battery capacity might be required to reduce waste. However, this will come with a higher initial investment and replacement cost.

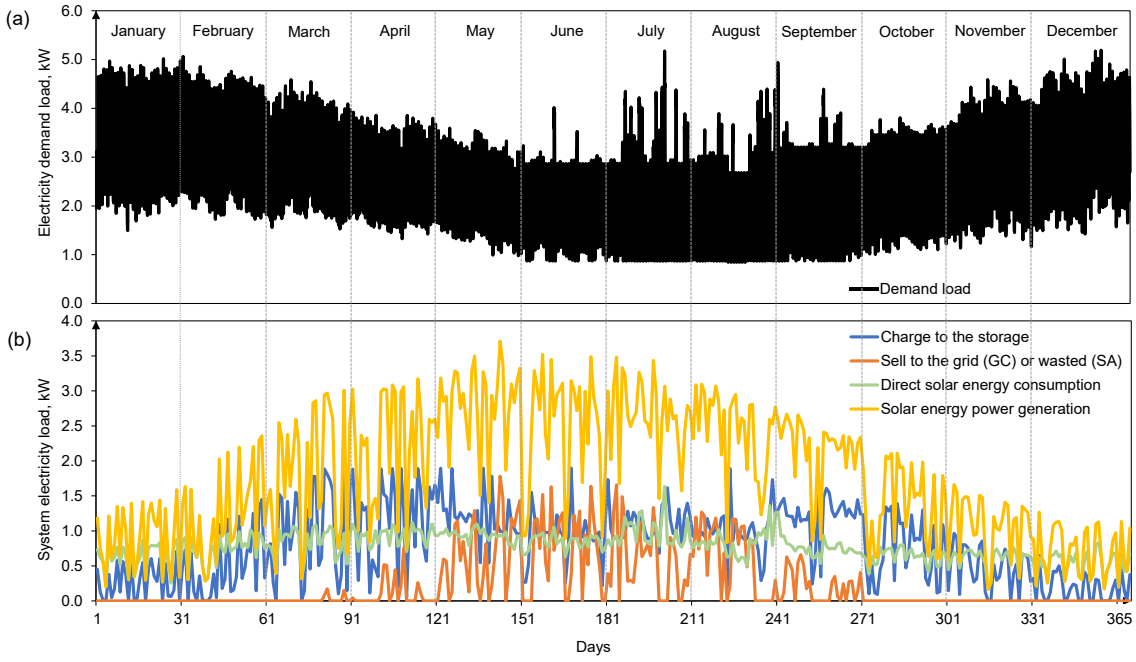

Figure 5. (a) Annual electricity demand load profile of the selected house; (b) Dynamic generated solar energy allocation of typical PV system from the model simulation

Figure 6 presents the percent demand met through solar energy for the prototype house when the panel and battery numbers changed. Either the number of panels or the number of batteries could be a limiting factor for further increase in percent demand met. The shaded numbers present where the PV array size serves as a primary limiting factor, while the rest presents where the battery size serves as a primary limiting factor. The borderline between the two sections represents the approximate optimized battery size to achieve the highest possible percentage of demand met with a given array size. Achieving 100% demand met requires large numbers of both panels (>200 units) and batteries (>160 units), which often accompanies a high cost.

However, the size of 40 panels (1.63 m^2/panel, 65.2 m^2 in total) already occupies the entire available roof size of the prototype house (65 m^2). Urban PV hosts are likely be more restricted by the land or space available for further increasing demand met compared to rural or suburban PV hosts. An integration of multiple decentralized energy supplies, such as PV and diesel generator, or PV and geothermal energy might be desirable to improve demand met.

Number of Panels \ Number of Batteries	0	1	5	10	15	20	40	80	160	320
1	1.6%	1.6%	1.6%	1.6%	1.6%	1.6%	1.6%	1.6%	1.6%	1.6%
5	8.1%	8.1%	8.1%	8.1%	8.1%	8.1%	8.1%	8.1%	8.1%	8.1%
10	15.8%	16.1%	16.1%	16.1%	16.1%	16.1%	16.1%	16.1%	16.1%	16.1%
15	21.2%	22.0%	23.5%	23.7%	23.7%	23.7%	23.7%	23.7%	23.7%	23.7%
20	24.9%	26.0%	29.0%	30.8%	31.0%	31.0%	30.9%	30.9%	30.9%	30.9%
25	27.6%	28.9%	32.7%	36.1%	37.7%	38.0%	38.0%	38.0%	38.0%	38.0%
30	29.7%	31.1%	35.4%	39.7%	42.8%	44.4%	44.9%	44.9%	44.9%	44.9%
35	31.2%	32.8%	37.7%	42.4%	46.4%	49.3%	51.4%	51.7%	51.7%	51.7%
40	32.5%	34.1%	39.4%	44.7%	49.1%	52.9%	56.2%	57.1%	57.6%	58.3%
60	35.8%	37.5%	43.6%	50.5%	56.6%	61.6%	68.4%	69.8%	70.2%	70.9%
80	37.8%	39.5%	45.9%	53.4%	60.4%	66.6%	75.4%	77.8%	78.8%	79.5%
100	39.1%	40.9%	47.4%	55.2%	62.7%	69.3%	80.7%	83.6%	84.4%	85.2%
150	41.0%	42.8%	49.6%	57.7%	65.7%	72.9%	87.2%	92.2%	93.3%	94.1%
200	42.0%	43.8%	50.7%	59.2%	67.3%	74.5%	89.9%	96.2%	98.4%	99.2%
300	43.2%	45.1%	52.0%	60.5%	69.1%	76.5%	92.5%	98.7%	99.9%	99.9%

Figure 6. Percentage of demand met via solar PV systems

3.2 Life cycle cost assessment

The life cycle cost of the baseline SA system is -$754.9 in 2018 value with 18.5 years of IPBT, while the baseline GC system presents a lower life cycle cost of -$1,739.4 with 16.8 years of IPBT. Our IPBTs found in this study are within the IPBT range of 2.8-40.8 years reported by previous residential solar PV studies (Muhammad-Sukki et al., 2014; Yang et al., 2015). Allowing selling of the surplus energy created about $984.5 of additional savings over 20 years of life span. In our simulation, to further increase 1% of the

percent demand met from baseline system would result in an additional $409.0 through the increase of array size or $626.5 through the increase of battery size. Both are higher than the amount of economic savings that can be achieved through the 1% demand met increase ($31.3).

Figure 7 presents the cost breakdowns of the baseline SA and GC PV systems. Primary costs for solar PV systems come from panels and racking (31% of total cost), battery storage (27% of total cost), replacement of battery (23% of total cost), and labor for installation (16% of total cost). Without system rebate and tax credit, both systems are not able to be paid back within its life time.

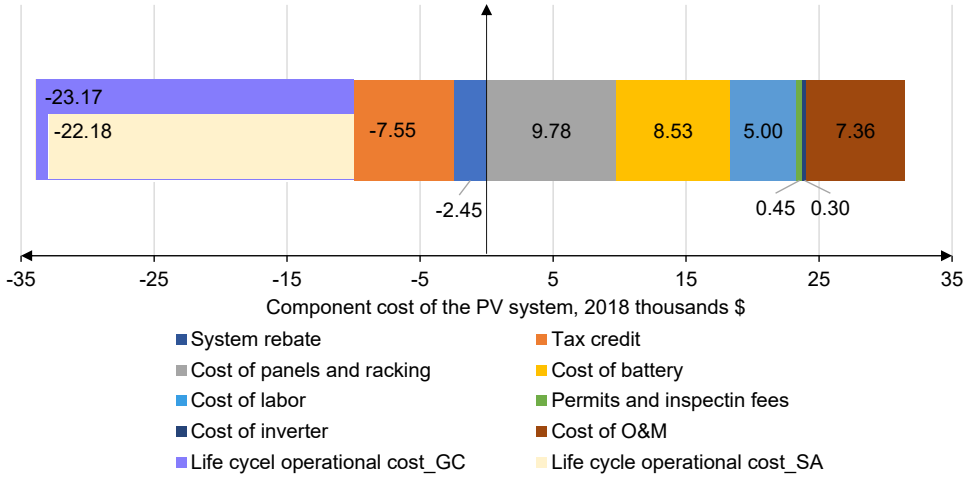

Figure 7. Cost breakdown of baseline 40-panel 40-battery SA and GC PV systems

Figure 8 presents the life cycle cost under different array sizes for the prototype house. Results show that when demand met is not a concern, life cycle economic savings are achievable under a range of panel and battery sizes for both GC and SA systems. No battery installation is preferred for SA systems with relatively small panel sizes (<25 panels). This indicates the saving from power generation cannot offset the battery cost within this range of panel sizes. With further increase in array size, the optimum battery size increases. Overall, the maximum life cycle economic saving can be achieved with 20 panels with no battery in this prototype house. This optimum configuration could meet ~25% of total demand with NPV of -$4,616.7. Compared with the baseline SA system, this optimized SA system increases the life cycle economic savings

by 511.6%, yet decreases the demand met by 55.7%. Additional analyses were conducted to investigate the tradeoffs between percent demand met and life cycle cost. The Pareto-optimal frontier between percent demand met and life cycle cost was provided in Figure 9 (further analyses related to the tradeoffs between the life cycle cost and demand met were provided in Figure S4 of the supporting information). We found the optimal panel size ranges from 60-80 with 20-40 batteries, which can meet 66.6-68.4% of the demand with a life cycle cost between -$3011.7 and -$887.5.

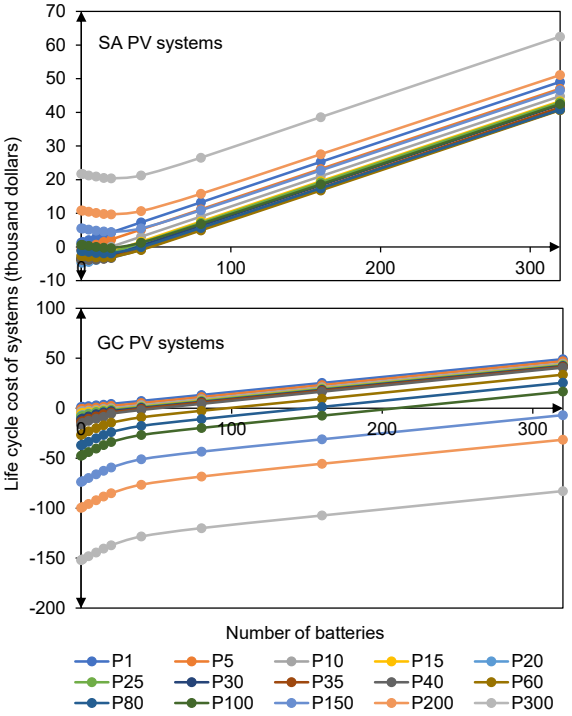

Figure 8. Life cycle cost (2018$) of SA and GC PV systems under different array sizes

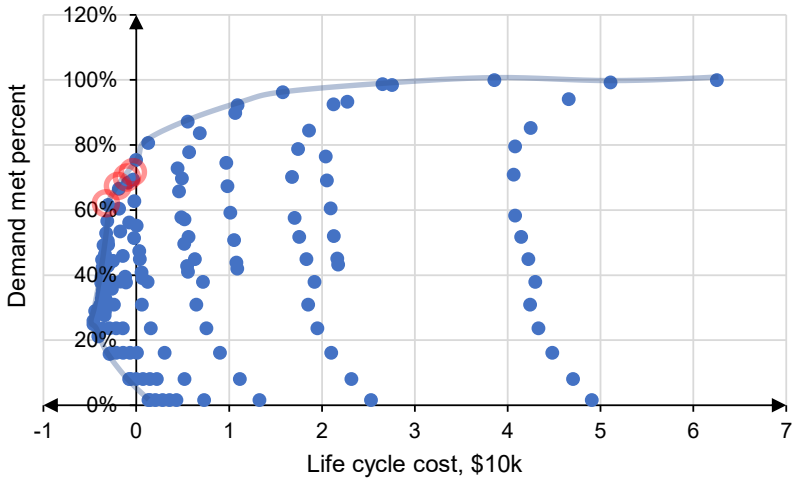

Figure 9. The Pareto-optimal front of demand met percent and life cycle cost of SA PV systems. Dots with red circles represent the preferred solutions for both objectives.

For GC systems, with a given array size, the life cycle cost increases with the increase of battery size. When there is no limit on when and how much excess solar energy can be sold to the grid, batteries do not provide extra benefit to the GC system owners. However, when policy constraints such as limitations/caps of grid sell are in place, tradeoffs would present as whether or not to install batteries for excess energy storage. For example, Pennsylvania Public Utility Commission attempted to cap the amount of surplus grid sell from PV systems to no more than 200% of residential customers' annual consumption over the 60 months before they installed PV systems (Legere, 2016; Parrish, 2016). Under such a policy, the prototype house with the baseline system would have a maximum grid sell of 39,080 kWh annually. With the decrease of the selling cap, this could result in a larger optimal battery storage capacity. Potential future charges on distribution and transmission services, overage tariffs, and a lower retail rate of solar energy can also influence the optimal sizing of the panels and batteries of the GC PV systems. In these conditions, storing the surplus solar energy for later household uses will result in a higher economic benefit than selling it directly back to the grid. Hence, having certain battery storage capacities might become appealing even for GC PV system owners. Different policies could alter the economic cost and benefit of GC systems through the change of

435 economic gain from selling to the grid variously. Therefore, the optimal array size for maximum economic
436 saving is determined by specific policy. For example, the cap of grid sell restricts the optimum array size.
437
438 3.3 Life cycle environmental assessment
439 Both baseline GC and SA PV systems can result in reduced CED, carbon footprint, and water footprint
440 compared to the grid when installed in the prototype house. The GC system has higher life cycle
441 environmental benefits in terms of all three measures than the SA system (-2.1 TJ, -177.0 Mg CO_2 eq, and
442 -9.4 ML of water for the SA system and -2.3 TJ, -187.0 Mg CO_2 eq, and -9.9 ML of water for the GC
443 system). This shows that allowing selling of the excess energy rather than wasting it can slightly increase
444 the environmental benefits by 5.3~9.5% over 20 years of life span. The energy, carbon, and water payback
445 times are 2.15, 1.62, and 0.65 years for the baseline SA system, respectively; and 2.05, 1.54, and 0.62 years
446 for the baseline GC system, respectively. Previously reported energy, carbon, and water payback times are
447 0.8-4.7 years (Gerbinet et al., 2014; Grant and Hicks, 2020; Perez et al., 2012), 0.4-7.8 years (Grant and
448 Hicks, 2020), and 0.06-1.08 years (Fthenakis and Kim, 2010; Meldrum et al., 2013) respectively for the
449 solar PV systems. Our results are within the ranges of these previously reported environmental payback
450 times. Figure 10 presents the life cycle environmental performances of SA and GC systems under different
451 array sizes. Compared with life cycle enconomic savings, life cycle environmental savings are achievable
452 under a wider range of panel and battery sizes for both types of systems.
453
454 For SA systems, the optimized CED and carbon footprint outcomes were achieved when the panel size was
455 in the range of 150-200 units and the battery size was in the range of 80-320 units, while the optimized
456 water footprint outcome was achieved when the panel size was in the range of 150-300 units and the battery
457 size was in the range of 80-320 units when installed in the prototype house. The optimized CED, carbon
458 footprint, and water footprint are in the ranges of -3.02 and -2.85 TJ, -262.2 and -254.0 Mg CO_2 eq, and -
459 15.4 and -14.7 ML of water, respectively. These optimized configurations increase the life cycle
460 environmental savings of the baseline SA system by up to 64.6%, but decrease the life cycle economic

461 saving largely by up to 6,868.4%. The environmentally optimal SA system array and battery sizes are
462 significantly larger than the economically optimal array and battery sizes. This large preferred size is
463 potentially a result of the relatively low environmental emissions/impacts during the panel and battery
464 manufacturing phase compared with the potential environmental benefits resulted from preventing the use
465 of the grid during the use phase, although a large amount of solar energy will be wasted under the optimized
466 size (up to 69.3% of total solar energy generation wasted). This shows that an environmental and economic
467 tradeoff exists for the SA systems. However, with further reductions in the capital costs of the PV and
468 battery systems, such tradeoffs may be minimized, especially for regions with relatively high retail
469 electricity price. Potential future policies such as carbon pricing (Tierney, 2019) and increased water pricing
470 of the thermal power supply (EPA, 2019; USC, 1986) may also help promoting adoption of larger sized
471 solar PV and battery systems as well as minimizing the environmental and economic tradeoffs.
472
473 For GC systems, environmental benefits are the highest when no battery is installed, and the benefits
474 increase with the increase of panel size. However, the increase of array size is restricted by the amount of
475 rooftop area or land availablibility. When the panel size is restricted to the rooftop area, the lowest life cycle
476 environmental costs in CED, carbon footprint, and water footprint are -2.5 TJ, -209.2 Mg CO_2 eq, and -
477 10.9 ML respectively. This optimized configuration increases the environmental and economic savings by
478 8.7~11.9% and 843.7% respectively compared with the baseline GC system over 20 years. No outstanding
479 economic and environmental tradeoffs were found for the GC system under the modelled conditions.

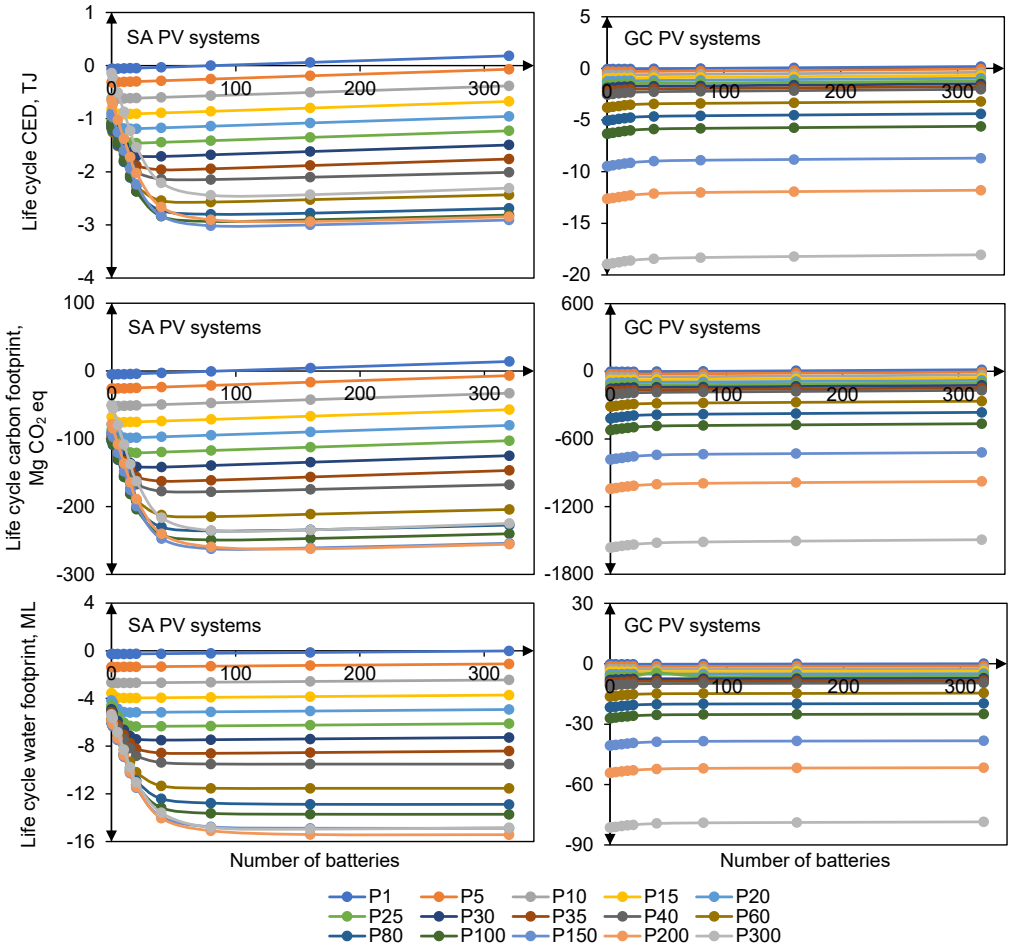

Figure 10. Life cycle environmental costs of SA and GC PV systems under different array sizes

3.4 Sensitivity analysis

Figure 11 shows the changes of the life cycle cost in response to decreases or increases of the discount rate as well as the changes of the life cycle environmental outcomes in response to the changes in the grid energy, carbon, and water intensities. Life cycle cost of the baseline PV system is highly sensitive to the changes of the discount rate under the investigated range. Increasing discount rate is associated with lower life cycle economic savings from installing solar panels. The discount rate of 5.6% (12% increase from the default value) and 6.3% (26% increase from the default value) are the tipping points where a SA and GC baseline system starts to lose money, respectively. Life cycle environmental outcomes of the solar PV system change linearly with the change of the grid energy, carbon, and water intensities. Carbon footprint has the highest

sensitivity to the changes in the grid, followed by water footprint, and the CED is the least sensitive to the grid changes. Additionally, the GC system is slightly more sensitive to changes in the grid than the SA system from an environmental perspective.

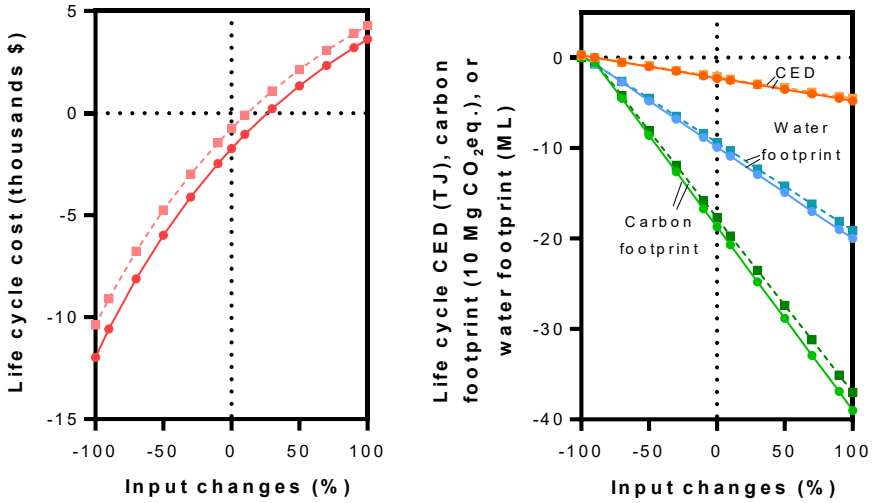

Figure 11. Life cycle costs and environmental impacts of the baseline SA (dashed lines) and GC (solid lines) PV system under changes in discount rate (left figure) and the unit environmental impact of the grid (right figure).

4. Conclusion

A dynamic life cycle economic and environmental assessment that combines system dynamics modeling with the conventional LCA and LCCA was conducted for residential solar PV systems. Two PV system designs were investigated: the GC and the SA systems. A prototype house located in Boston, MA was used as a testbed for the modeling framework developed in this study. When installed with 40 PV panels (roughly the size of the entire roof) and 40 batteries, the prototype house will directly use 42.6% of the solar energy generated, store 44.4% of the energy for later consumption, and sell or waste round 13.0% of the solar energy depending on whether it is a GC or a SA system. Solar energy generated, stored, and sold/wasted all present strong seasonal trends. The prototype house has the lowest monthly demand during summer, while the solar energy generation is the highest during the period. Hence, a larger amount of solar energy

can be sold or stored during these months. Achieving 100% demand met requires large numbers of both panels (>200 units) and batteries (>160 units) for the prototype house, which can be unrealistic for households with land or roof area availabilities. The 40-panel 40-battery SA system has a life cycle cost saving of $754.9 in 2018 value with 18.5 years of IPBT and a life cycle reduction of 2.1 TJ of CED, 177.0 Mg CO_2 eq, and 9.4 ML of water. The corresponding GC system presents a slightly higher life cycle cost saving of $1,739.4 with 16.8 years of IPBT and a slightly higher life cycle environmental benefit (reduction of 2.3 TJ CED, 187.0 Mg CO_2 eq, and 9.9 ML of water). This study also found the tradeoffs between demand met and life cycle cost in the SA systems can be best balanced when the panel size is between 60-80 units and the battery size is between 20-40 units, which can meet 66.6-68.4% of the demand with a life cycle cost between -$3011.7 and -$887.5.

When examining the influence of panel and battery sizes on the outcome, we found life cycle economic savings are achievable under a range of panel and battery sizes for both GC and SA systems when demand met is not a concern. For the SA systems, the maximum life cycle economic saving can be achieved with 20 panels with no battery in the prototype house, which increases the life cycle economic savings of the baseline system by 511.6%, yet decreases the demand met by 55.7%. However, the optimized environmental performance is achieved with significantly larger panel (up to 300 units) and battery (up to 320 units) sizes. These optimized configurations increase the life cycle environmental savings of the baseline SA system by up to 64.6%, but decrease the life cycle economic saving largely by up to 6,868.4%. There is a clear environmental and economic tradeoff when selecting the size of the SA systems. For GC systems, when there is no limit on when and how much excess solar energy can be sold to the grid, batteries do not provide extra benefit to the GC system owners. Hence, both the economic and environmental benefits are the highest when no battery is installed, and the benefits increase with the increase of panel size. However, when policy constraints such as limitations/caps of grid sell are in place, tradeoffs would present as whether or not to install batteries for excess energy storage. The modeling framework that is developed

in this study can be further generalized for future investigations in varied PV system designs under different policy scenarios in different spatial and temporal contexts.

Acknowledgements

We acknowledge the National Science Foundation's support via a CBET award (#1706143) and a CRISP Type I Award (#1638334). The views, findings, and conclusions expressed in this study are those of the authors and do not necessarily reflect the views of the National Science Foundation.

References

Abu-jasser, A., 2010. a Stand-Alone Photovoltaic System , Case Study : a Residence in Gaza. Appl. Sci. Environ. Sanit. 5, 81–91.

Adriana, C., Antošová, M., Andrea, S., Čulková, K., 2012. Economical Analysis of the Photovoltaic Systems - Case Study Slovakia. AASRI Procedia 2, 186–191. https://doi.org/10.1016/j.aasri.2012.09.033

Akinyele, D.O., Rayudu, R.K., 2016a. Comprehensive techno-economic and environmental impact study of a localised photovoltaic power system (PPS) for off-grid communities. Energy Convers. Manag. 124, 266–279. https://doi.org/10.1016/j.enconman.2016.07.022

Akinyele, D.O., Rayudu, R.K., 2016b. Techno-economic and life cycle environmental performance analyses of a solar photovoltaic microgrid system for developing countries. Energy 109, 160–179. https://doi.org/10.1016/j.energy.2016.04.061

Akinyele, D.O., Rayudu, R.K., Nair, N.K.C., 2017. Life cycle impact assessment of photovoltaic power generation from crystalline silicon-based solar modules in Nigeria. Renew. Energy 101, 537–549. https://doi.org/https://doi.org/10.1016/j.renene.2016.09.017

Allouhi, A., Saadani, R., Buker, M.S., Kousksou, T., Jamil, A., Rahmoune, M., 2019. Energetic, economic and environmental (3E) analyses and LCOE estimation of three technologies of PV grid-connected systems under different climates. Sol. Energy 178, 25–36. https://doi.org/10.1016/j.solener.2018.11.060

Allouhi, A., Saadani, R., Kousksou, T., Saidur, R., Jamil, A., Rahmoune, M., 2016. Grid-connected PV systems installed on institutional buildings: Technology comparison, energy analysis and economic performance. Energy Build. 130, 188–201. https://doi.org/10.1016/j.enbuild.2016.08.054

Association, N.M., 2015. C&I Solar Rebate Program [WWW Document]. URL https://www.nhmunicipal.org/Resources/ViewDocument/419

Azzopardi, B., Mutale, J., 2010. Life cycle analysis for future photovoltaic systems using hybrid solar cells. Renew. Sustain. Energy Rev. 14, 1130–1134.

https://doi.org/https://doi.org/10.1016/j.rser.2009.10.016

Bernal-Agustín, J.L., Dufo-López, R., 2006. Economical and environmental analysis of grid connected photovoltaic systems in Spain. Renew. energy 31, 1107–1128. https://doi.org/10.1016/j.renene.2005.06.004

Berwal, A.K., Kumar, S., Kumari, N., Kumar, V., Haleem, A., 2017. Design and analysis of rooftop grid tied 50 kW capacity Solar Photovoltaic (SPV) power plant. Renew. Sustain. Energy Rev. 77, 1288–1299. https://doi.org/10.1016/j.rser.2017.03.017

Bortolini, M., Gamberi, M., Graziani, A., 2014. Technical and economic design of photovoltaic and battery energy storage system. Energy Convers. Manag. 86, 81–92. https://doi.org/10.1016/j.enconman.2014.04.089

Boulay, A.-M., Bare, J., Benini, L., Berger, M., Lathuillière, M.J., Manzardo, A., Margni, M., Motoshita, M., Núñez, M., Pastor, A.V., 2018. The WULCA consensus characterization model for water scarcity footprints: assessing impacts of water consumption based on available water remaining (AWARE). Int. J. Life Cycle Assess. 23, 368–378.

Burns, J.E., Kang, J.-S.S., 2012. Comparative economic analysis of supporting policies for residential solar PV in the United States: Solar Renewable Energy Credit (SREC) potential. Energy Policy 44, 217–225. https://doi.org/10.1016/j.enpol.2012.01.045

Chandel, M., Agrawal, G.D., Mathur, S., Mathur, A., 2014. Techno-economic analysis of solar photovoltaic power plant for garment zone of Jaipur city. Case Stud. Therm. Eng. 2, 1–7. https://doi.org/10.1016/j.csite.2013.10.002

Connolly, D., Lund, H., Mathiesen, B.V., Leahy, M., 2010. A review of computer tools for analysing the integration of renewable energy into various energy systems. Appl. Energy 87, 1059–1082.

Curry, C., 2017. Lithium-ion battery costs and market. Bloom. New Energy Financ. 5.

De Souza, M.A., Farias, F.S., Costa, J.C.W.A., Cardoso, D.L., 2017. Technical Economic Analysis of Photovoltaic Systems in Heterogeneous Mobile Networks. Procedia Comput. Sci. 109, 825–832. https://doi.org/10.1016/j.procs.2017.05.346

Devices—Part, P., 1AD. Measurement of Photovoltaic Current-Voltage Characteristics. CEI/IEC 60901–60904.

DOE, n.d. United States Department of Energy, Solar Energy Potential [WWW Document]. Natl. Renew. Energy Lab. URL https://www.energy.gov/maps/solar-energy-potential

Duffie, J.A., Beckman, W.A., 1991. Radiation characteristics of opaque materials. Sol. Eng. Therm. Process. 184.

EIA, 2019a. U.S. Energy Information Administration, Electricity explained, Electricity in the United States [WWW Document]. URL https://www.eia.gov/energyexplained/electricity/electricity-in-the-us.php

EIA, 2019b. U.S. Energy Information Administration, Electric Power Monthly [WWW Document]. URL https://www.eia.gov/electricity/monthly/epm_table_grapher.php?t=epmt_1_17_a

EIA, 2019c. U.S. Energy Information Administration, Electric Power Monthly [WWW Document]. URL https://www.eia.gov/electricity/monthly/#generation

EIA, 2017. Institute for 21st Century Energy, U.S. CHAMBER OF COMMERCE, 2016 U.S. Average Electricity Retail Prices [WWW Document]. U.S. Energy Inf. Adm. Electr. Power Mon. 2017. URL https://www.globalenergyinstitute.org/sites/default/files/023162_EI21_AverageElectricRetail_Map_2016 Final.pdf

EIA, 2011. U.S. Energy Information Administration, Electricity demand changes in predictable patterns [WWW Document]. URL https://www.eia.gov/todayinenergy/detail.php?id=4190

Eid, C., Guillén, J.R., Marín, P.F., Hakvoort, R., 2014. The economic effect of electricity net-metering with solar PV: Consequences for network cost recovery, cross subsidies and policy objectives. Energy Policy 75, 244–254.

Elhodeiby, A.S., Metwally, H.M.B., Farahat, M.A., 2011. performance analysis of 3.6 kW roof top grid connected photovoltaic system in egypt, in: International Conference on Energy Systems and Technologies (ICEST 2011), Cairo, Egypt. pp. 11–14.

EPA, 2019. United States Environmental Protection Agency, Electric Power Generation, Transmission

620 and Distribution (NAICS 2211) [WWW Document]. URL https://www.epa.gov/regulatory-
621 information-sector/electric-power-generation-transmission-and-distribution-naics-2211
622 Eversource, 2018. Eversource, Massachusetts Application to Connect [WWW Document]. URL
623 https://www.eversource.com/content/ct-c/about/about-us/doing-business-with-us/builders-
624 contractors/interconnections/massachusetts-application-to-connect
625 Faiman, D., 2008. Assessing the outdoor operating temperature of photovoltaic modules. Prog.
626 Photovoltaics Res. Appl. 16, 307–315.
627 Ford, A., Ford, F.A., 1999. Modeling the environment: an introduction to system dynamics models of
628 environmental systems. Island press.
629 Forrester, J.W., 1997. Industrial dynamics. J. Oper. Res. Soc. 48, 1037–1041.
630 Fthenakis, V., Kim, H.C., 2010. Life-cycle uses of water in U.S. electricity generation. Renew. Sustain.
631 Energy Rev. 14, 2039–2048. https://doi.org/10.1016/J.RSER.2010.03.008
632 Fthenakis, V.M., Kim, H.C., 2011. Photovoltaics: Life-cycle analyses. Sol. Energy 85, 1609–1628.
633 https://doi.org/10.1016/j.solener.2009.10.002
634 Fu, R., Margolis, R.M., Feldman, D.J., 2018. US Solar Photovoltaic System Cost Benchmark: Q1 2018.
635 National Renewable Energy Lab.(NREL), Golden, CO (United States).
636 García, M.C.A., Balenzategui, J.L., 2004. Estimation of photovoltaic module yearly temperature and
637 performance based on nominal operation cell temperature calculations. Renew. energy 29, 1997–
638 2010.
639 Gerbinet, S., Belboom, S., Léonard, A., 2014. Life Cycle Analysis (LCA) of photovoltaic panels: A
640 review. Renew. Sustain. Energy Rev. 38, 747–753. https://doi.org/10.1016/j.rser.2014.07.043
641 Grant, C.A., Hicks, A.L., 2020. Effect of manufacturing and installation location on environmental impact
642 payback time of solar power. Clean Technol. Environ. Policy 22, 187–196.
643 Grinenko, T., 2018. Solar Panel Recycling 101 [WWW Document]. URL
644 https://www.renvu.com/Learn/Solar-Panel-Recycling-101
645 Gürtürk, M., 2019. Economic feasibility of solar power plants based on PV module with levelized cost

646 analysis. Energy 171, 866–878. https://doi.org/10.1016/j.energy.2019.01.090
647 Heeter, J., Gelman, R., Bird, L., 2014. Status of net metering: Assessing the potential to reach program
648 caps. National Renewable Energy Lab.(NREL), Golden, CO (United States).
649 HomeAdvisor, I., 2019. 2019 Solar Panel Cost Guide, Home Solar System Installation Prices [WWW
650 Document]. URL https://www.homeadvisor.com/cost/heating-and-cooling/install-solar-panels/
651 HOMER, 2018. HOMER Energy, HOMER Pro 3.11 [WWW Document]. URL
652 https://www.homerenergy.com/products/pro/docs/3.11/index.html
653 HOMER, 2017. HOMER Energy, HOMER Grid 1.1 [WWW Document]. URL
654 https://www.homerenergy.com/products/grid/docs/1.1/index.html
655 ISO-NE, 2018. ISO-New England, Energy, Load, and Demand Reports [WWW Document]. URL
656 https://www.iso-ne.com/isoexpress/web/reports/load-and-demand/-/tree/net-ener-peak-load
657 Jeong, Y.-C., Lee, E.-B., Alleman, D., 2019. Reducing voltage volatility with step voltage regulators: A
658 life-cycle cost analysis of Korean solar photovoltaic distributed generation. Energies 12, 652.
659 Jones, C., Peshev, V., Gilbert, P., Mander, S., 2018. Battery storage for post-incentive PV uptake? A
660 financial and life cycle carbon assessment of a non-domestic building. J. Clean. Prod. 167, 447–458.
661 https://doi.org/10.1016/j.jclepro.2017.08.191
662 Kaundinya, D.P., Balachandra, P., Ravindranath, N.H., 2009. Grid-connected versus stand-alone energy
663 systems for decentralized power—A review of literature. Renew. Sustain. Energy Rev. 13, 2041–
664 2050. https://doi.org/https://doi.org/10.1016/j.rser.2009.02.002
665 Kazem, H.A., Albadi, M.H., Al-Waeli, A.H.A., Al-Busaidi, A.H., Chaichan, M.T., 2017. Techno-
666 economic feasibility analysis of 1MW photovoltaic grid connected system in Oman. Case Stud.
667 Therm. Eng. 10, 131–141. https://doi.org/10.1016/j.csite.2017.05.008
668 Koehl, M., Heck, M., Wiesmeier, S., Wirth, J., 2011. Modeling of the nominal operating cell temperature
669 based on outdoor weathering. Sol. Energy Mater. Sol. Cells 95, 1638–1646.
670 Köntges, M., Altmann, S., Heimberg, T., Jahn, U., Berger, K.A., 2016. Mean degradation rates in PV
671 systems for various kinds of PV module failures, in: Proc. of the 32nd European Photovoltaic Solar

672 Energy Conference and Exhibition, München: WIP. pp. 1435–1443.
673 Kottek, M., Grieser, J., Beck, C., Rudolf, B., Rubel, F., 2006. World map of the Köppen-Geiger climate
674 classification updated. Meteorol. Zeitschrift 15, 259–263.
675 Lai, C.S., McCulloch, M.D., 2017. Levelized cost of electricity for solar photovoltaic and electrical
676 energy storage. Appl. Energy 190, 191–203. https://doi.org/10.1016/j.apenergy.2016.12.153
677 Leckner, M., Zmeureanu, R., 2011. Life cycle cost and energy analysis of a Net Zero Energy House with
678 solar combisystem. Appl. Energy 88, 232–241. https://doi.org/10.1016/j.apenergy.2010.07.031
679 Lee, M., Hong, T., Jeong, K., Kim, J., 2018. A bottom-up approach for estimating the economic potential
680 of the rooftop solar photovoltaic system considering the spatial and temporal diversity. Appl. Energy
681 232, 640–656. https://doi.org/10.1016/j.apenergy.2018.09.176
682 Legere, L., 2016. Government Technology, Pennsylvania PUC Drops Net-Metering Cap for Alternate
683 Energy Users [WWW Document]. URL https://www.govtech.com/fs/Pennsylvania-PUC-Drops-
684 Net-Metering-Cap-for-Alternate-Energy-Users.html
685 M. Raugei, M.S.. F.R.I.P.S.M. de W.-S.J.Z.V.F.H.C.K., 2015. Life Cycle Inventories and Life Cycle
686 Assessments of Photovoltaic Systems Life Cycle Inventories and Life Cycle Assessments of
687 Photovoltaic Systems.
688 Manwell, J.F., McGowan, J.G., 1993. Lead acid battery storage model for hybrid energy systems. Sol.
689 Energy 50, 399–405.
690 McFarland, E.W., 2014. Solar energy: setting the economic bar from the top-down. Energy Environ. Sci.
691 7, 846–854.
692 Meldrum, J., Nettles-Anderson, S., Heath, G., Macknick, J., 2013. Life cycle water use for electricity
693 generation: a review and harmonization of literature estimates. Environ. Res. Lett. 8, 15031.
694 Muhammad-Sukki, F., Abu-Bakar, S.H., Munir, A.B., Mohd Yasin, S.H., Ramirez-Iniguez, R.,
695 McMeekin, S.G., Stewart, B.G., Sarmah, N., Mallick, T.K., Abdul Rahim, R., Karim, M.E., Ahmad,
696 S., Mat Tahar, R., 2014. Feed-in tariff for solar photovoltaic: The rise of Japan. Renew. Energy 68,
697 636–643. https://doi.org/10.1016/J.RENENE.2014.03.012

698 Muñoz-García, M.A., Marin, O., Alonso-García, M.C., Chenlo, F., 2012. Characterization of thin film PV
699 modules under standard test conditions: Results of indoor and outdoor measurements and the effects
700 of sunlight exposure. Sol. Energy 86, 3049–3056.
701 Nelson, D.B., Nehrir, M.H., Wang, C., 2006. Unit sizing and cost analysis of stand-alone hybrid
702 wind/PV/fuel cell power generation systems. Renew. Energy 31, 1641–1656.
703 https://doi.org/https://doi.org/10.1016/j.renene.2005.08.031
704 NREL, 2017. National Renewable Energy Laboratory, Sustainable Energy, PVWatts® Calculator [WWW
705 Document]. URL https://pvwatts.nrel.gov/index.php
706 NREL, 2015. National Renewable Energy Laboratory, National Solar Radiation Database [WWW
707 Document]. URL https://rredc.nrel.gov/solar/old_data/nsrdb/
708 NREL, 2014. National Renewable Energy Laboratory, U.S. Department of Energy, Commercial and
709 Residential Hourly Load Profiles for all TMY3 Locations in the United States [WWW Document].
710 URL https://openei.org/datasets/files/961/pub/
711 Parida, B., Iniyan, S., Goic, R., 2011. A review of solar photovoltaic technologies. Renew. Sustain.
712 energy Rev. 15, 1625–1636. https://doi.org/10.1016/j.rser.2010.11.032
713 Parrish, T., 2016. PUC Approves Cap on Home-Produced Energy Sold to Grid [WWW Document]. URL
714 https://www.mcall.com/mc-pa-resale-electricity-20160214-story.html
715 Peng, J., Lu, L., Yang, H., 2013. Review on life cycle assessment of energy payback and greenhouse gas
716 emission of solar photovoltaic systems. Renew. Sustain. Energy Rev. 19, 255–274.
717 https://doi.org/10.1016/j.rser.2012.11.035
718 Perez, M.J.R., Fthenakis, V., Kim, H., Pereira, A.O., 2012. Façade–integrated photovoltaics: a life cycle
719 and performance assessment case study. Prog. Photovoltaics Res. Appl. 20, 975–990.
720 Poullikkas, A., 2013. A comparative assessment of net metering and feed in tariff schemes for residential
721 PV systems. Sustain. Energy Technol. Assessments 3, 1–8.
722 https://doi.org/https://doi.org/10.1016/j.seta.2013.04.001
723 Rawat, B.S., Negi, P., Pant, P.C., Joshi, G.C., 2018. Evaluation of energy yield ratio (EYR), energy

724 payback period (EPBP) and GHG-emission mitigation of solar home lighting PV-systems of 37Wp
725 modules in India. Int. J. Renew. Energy Res. 8.
726 Rebitzer, G., Ekvall, T., Frischknecht, R., Hunkeler, D., Norris, G., Rydberg, T., Schmidt, W.-P., Suh, S.,
727 Weidema, B.P., Pennington, D.W., 2004. Life cycle assessment: Part 1: Framework, goal and scope
728 definition, inventory analysis, and applications. Environ. Int. 30, 701–720.
729 Reichelstein, S., Yorston, M., 2013. The prospects for cost competitive solar PV power. Energy Policy
730 55, 117–127.
731 SEIA, 2019. Solar Energy Industries Association, U.S. Solar Market Insight [WWW Document]. URL
732 https://www.seia.org/us-solar-market-insight
733 Service, U.S.I.R., 2019. Residential Renewable Energy Tax Credit [WWW Document]. URL
734 https://www.energy.gov/savings/residential-renewable-energy-tax-credit
735 Sharma, S., Jain, K.K., Sharma, A., 2015. Solar Cells: In Research and Applications—A Review. Mater.
736 Sci. Appl. 06, 1145–1155. https://doi.org/10.4236/msa.2015.612113
737 Shea, R.P., Worsham, M.O., Chiasson, A.D., Kelly Kissock, J., McCall, B.J., 2020. A lifecycle cost
738 analysis of transitioning to a fully-electrified, renewably powered, and carbon-neutral campus at the
739 University of Dayton. Sustain. Energy Technol. Assessments 37, 100576.
740 https://doi.org/10.1016/J.SETA.2019.100576
741 SNL, 2018. Sandia National Laboratories, National Technology and Engineering Solutions of Sandia,
742 Sandia Module Temperature Model [WWW Document]. URL https://pvpmc.sandia.gov/modeling-
743 steps/2-dc-module-iv/module-temperature/sandia-module-temperature-model/
744 Song, C., Omalley, A., Roy, S.G., Barber, B.L., Zydlewski, J., Mo, W., 2019. Managing dams for energy
745 and fish tradeoffs: What does a win-win solution take? Sci. Total Environ. 669, 833–843.
746 https://doi.org/10.1016/j.scitotenv.2019.03.042
747 Spanos, C., Turney, D.E., Fthenakis, V., 2015. Life-cycle analysis of flow-assisted nickel zinc-,
748 manganese dioxide-, and valve-regulated lead-acid batteries designed for demand-charge reduction.
749 Renew. Sustain. Energy Rev. 43, 478–494.

Sterman, J.D., 2000. Business dynamics: systems thinking and modeling for a complex world.

Tierney, S., 2019. Clean Energy in New York State: The Role and Economic Impacts of a Carbon Price in NYISO's Wholesale Electricity Markets.

Tsang, M.P., Sonnemann, G.W., Bassani, D.M., 2016. Life-cycle assessment of cradle-to-grave opportunities and environmental impacts of organic photovoltaic solar panels compared to conventional technologies. Sol. Energy Mater. Sol. Cells 156, 37–48. https://doi.org/10.1016/j.solmat.2016.04.024

Uddin, K., Gough, R., Radcliffe, J., Marco, J., Jennings, P., 2017. Techno-economic analysis of the viability of residential photovoltaic systems using lithium-ion batteries for energy storage in the United Kingdom. Appl. Energy 206, 12–21. https://doi.org/10.1016/j.apenergy.2017.08.170

USC, 1986. The United States Congress, Electric Consumers Protection Act of 1986, United States [WWW Document]. URL https://www.usbr.gov/power/legislation/ecpa.pdf

Ventana Systems, I., 2015. Vensim Software [WWW Document]. URL http://vensim.com/vensim-software/

Verlinden, P., Yingbin, Z., Zhiqiang, F., 2013. Cost analysis of current PV production and strategy for future silicon PV modules, in: 28th European Photovoltaic Conference and Exhibition, Paris.

Wilson, E., Engebrecht Metzger, C.., Horowitz, S., Hendron, R., 2014. 2014 Building America House Simulation Protocols (NREL/TP-5500-60988).

Wu, P., Ma, X., Ji, J., Ma, Y., 2017. Review on Life Cycle Assessment of Greenhouse Gas Emission Profit of Solar Photovoltaic Systems. Energy Procedia 105, 1289–1294. https://doi.org/10.1016/j.egypro.2017.03.460

Xu, L., Zhang, S., Yang, M., Li, W., Xu, J., 2018. Environmental effects of China's solar photovoltaic industry during 2011–2016: A life cycle assessment approach. J. Clean. Prod. 170, 310–329. https://doi.org/10.1016/j.jclepro.2017.09.129

Yang, D., Latchman, H., Tingling, D., Amarsingh, A.A., 2015. Design and return on investment analysis of residential solar photovoltaic systems. IEEE Potentials 34, 11–17.

776 Zhang, X., Li, M., Ge, Y., Li, G., 2016. Techno-economic feasibility analysis of solar photovoltaic power
777 generation for buildings. Appl. Therm. Eng. 108, 1362–1371.
778 https://doi.org/10.1016/j.applthermaleng.2016.07.199
779
780